PERGAMON

International Journal of Heat and Mass Transfer 44 (2001) 1507–1515

International Journal of HEAT and MASS TRANSFER

www.elsevier.com/locate/ijhmt

A unified analysis of filling and solidification in casting with natural convection

Ik-Tae Im [a], Woo-Seung Kim [b,*], Kwan-Soo Lee [c]

[a] *Department of Automotive Engineering, Iksan National College, 194-5, Ma-dong Iksan, Chollabuk-do 570-752, South Korea*
[b] *Department of Mechanical Engineering, Hanyang University, 1271 Sa 1-dong, Ansan, Kyunggi-do 425-791, South Korea*
[c] *Department of Mechanical Engineering, Hanyang University, 17, Haengdang-dong Sungdong-gu, Seoul 133-791, South Korea*

Received 21 May 1999; received in revised form 7 June 2000

Abstract

In this paper, a unified model for simultaneous filling and solidification is applied to the two-dimensional filling and solidification of a square cavity. The effects of wall temperature and gate position on solidification are examined. The mixed natural-convection flow and residual flow resulting from the completion of filling are included in this study to investigate the coupled effects of filling and natural convection on solidification. Two different filling configurations (assisting flow and opposite flow due to the gate position) are analyzed to study the effects of residual flow on solidification. The results clearly show the necessity to carry out a coupled filling and solidification analysis, including the effect of natural convection. A numerical algorithm that uses the implicit volume of fluid (VOF) method for filling and a general, implicit, source-based method for solidification are presented.

1. Introduction

Casting processes are widely used to produce metal components. The demand for high precision casting parts continues to increase due to exacting demands from the automotive and aero-industries. Much research has been devoted toward process development for the production of high quality casting goods at low costs. From a macroscopic point of view, casting processes involve the coupling of solidification heat transfer and fluid flow. Three different flow mechanisms may be identified: (a) mold filling through the gating system, (b) residual flow due to the incoming momentum and (c) the natural-convection-driven flow in the mold can be considered during the casting process. From the heat transfer point of view, the solidification and thermal stresses due to shrinkage are important physical phenomena. Solidification includes the phase transition from a molten metal to a solid state due to heat removal from the mold/chill and segregation during solidification. The shapes of casting parts can become changed during the solidification process if there is severe thermal stress in the mold or in the casting part itself. These complicated physical phenomena during a casting process require complicated numerical methodologies. As a result, unrealistic restrictions are often imposed in order to render a model tractable.

The most widely studied area of casting is phase-change heat transfer [1,2]; natural convection effects [3,4] and macro/micro segregation [5] have only recently been studied in some detail. Fluid flow analysis during the mold filling process has been studied vigorously in recent decades due to the advent of computer hardware systems. The filling of a simple mold geometry has been previously modelled [6] and studies for an effective filling algorithm have also been reported [7–10].

Liquid metal cools as it flows into the mold. In the case of a thin cast part or a casting of molten metal with low superheat, the molten metal is cooled during filling and the molten metal is locally fully solidified before the mold is completely filled. Hence, it is necessary to simultaneously analyze the mold filling and solidification

* Corresponding author. Tel.: +82-345-400-5248; fax: +82-345-406-5550.
E-mail address: wskim@email.hanyang.ac.kr (W.-S. Kim).

0017-9310/01/$ - see front matter
PII: S0017-9310(00)00197-6

Nomenclature

a	discretization coefficient
b	constant term in discretization equation
d	coefficient in Eq. (10)
C	constant related to the solidification phase morphology
c	specific heat at constant pressure
F	volume of fluid function
f_l	volume fraction of liquid
G	modified volume of fluid function
$\boldsymbol{g}$	gravitational acceleration vector
H	total enthalpy
h_{sl}	latent heat
k	thermal conductivity
S_c	constant part of the source term, Eq. (13b)
S_p	source term, Eq. (13a)
T	temperature
t	time
$\boldsymbol{u}$	velocity vector
u, v	velocity component in x and y directions
x, y	Cartesian coordinates

Greek symbols

β	volumetric expansion coefficient
μ	viscosity of liquid metal
ρ	density

Subscripts

l	liquid
p	point under consideration
ref	reference
s	solid

Superscripts

$m, m+1$	iteration number
old	previous time

processes. Most of the previous works have considered only the solidification process after filling. Recently, the simultaneous analysis of mold filling and solidification phenomena has been reported. Wang and Perry [11] studied the filling characteristics in thin-wall investment castings as a function of parameters such as gate velocity, superheat of molten metal and mold pre-heat condition. Hu et al. [12] proposed a model for filling and solidification in a die-casting process. They assumed that the liquid metal was dispersed like droplets with air in the mold. Swaminathan and Voller [13] proposed a time-implicit, unified filling algorithm, which is not restricted to the Courant criterion inherent in the existing filling algorithms. Van Tol et al. [14] tested the simple boundary conditions at the gate or the choke instead of the full gating system such as runners and sprues in gravity casting systems.

In the mean time, Minaie et al. [15] analyzed natural-convection-driven flow and solidification in a casting process. They separated the process into two periods, that is, the filling period and the residual flow period after the mold was completely filled. They used the velocity field obtained from the ingate condition and continuity equation as an initial condition for the residual flow analysis and compared the interface shapes to the results from considering pure natural convection. In the benchmark test of the Seventh Conference on the Modeling of Casting, Welding and Advanced Solidification Process (MCWASP VII) [16], nine voluntary research groups took part and showed the present state-of-the-art of numerical simulation of the casting process. Most of the previous works, including those by MCWASP VII participants, considered the filling and solidification processes separately and did not combine the two. Full understanding of filling and heat transfer phenomena in casting processes requires an analysis that includes the effect of mold filling, residual flow after filling and the effect of the flow, due to natural convection, on the solidification process.

In this study, a simultaneous analysis model of the fluid flow and solidification during the entire casting process is developed. The model includes the residual flow due to the filling stage and the free convection in the mold. A simple casting model has been analyzed to consider their effects on the solidification phase change.

2. Mathematical modeling

Fluid flow during mold filling involves free surface flow. The subsequent solidification of the metal is a moving interface problem since the solidification front moves with time. If liquid metal is Newtonian and the flow is laminar, the governing equations for mass, momentum and energy conservation are as follows

$$\frac{\partial \rho}{\partial t} + \nabla \cdot [\rho \boldsymbol{u}] = 0, \tag{1}$$

$$\frac{\partial}{\partial t}[\rho \boldsymbol{u}] + \nabla \cdot [\rho \boldsymbol{u}\boldsymbol{u}] = \nabla \cdot [\mu \nabla \boldsymbol{u}] + S, \tag{2}$$

$$\frac{\partial}{\partial t}[\rho H] + \nabla \cdot [\rho \boldsymbol{u} H] = \nabla \cdot [k \nabla T], \tag{3}$$

where ρ is the density, t the time, μ the viscosity of the molten metal, k the thermal conductivity, H the total enthalpy and T the temperature, respectively. The source term S in the momentum equation, which must take

natural convection and solidification into account, is written as

$$S = -\frac{C(1-f_l)^2}{f_l^3}\boldsymbol{u} + \rho \boldsymbol{g}\beta(T - T_{\text{ref}}), \tag{4}$$

where C is the constant value related to the solidification phase morphology, $\boldsymbol{u}$ the velocity vector, f_l the liquid fraction and β is the volumetric expansion coefficient. The first term on the right-hand side of Eq. (4) mimics flow in a porous medium; dendrite structure of the solid interface is assumed in this study. This modeling technique has been validated experimentally in the melting problem of gallium [17].

It is expected that a laminar analysis will be sufficient for the problems to be investigated. While the initial pouring of molten metal into a mold undoubtedly involves some form of turbulence, this flow quickly becomes laminar due to the solidification. Indeed, the majority of previous works has also used this assumption [8,18]. Solute redistribution and segregation are important phenomena in an alloy solidification problem, but they are not considered here since they are beyond the scope of this study.

The velocity on the mold wall is zero in principle, but it is more realistic to use the free-slip boundary condition rather than a no-slip condition, where a rather coarse computational grid is used. In this study, the normal velocity at the mold wall boundaries is zero and the tangential velocity of the cells on the mold wall is equal to the fictitious wall velocity, which is parallel to the wall. It is, therefore, assumed that there is no friction on the wall for flow calculation.

2.1. Modified volume of fluid (VOF) method

During the mold filling process, liquid metal and air coexist in the mold and the interface position changes rapidly with time. It is thus essential to introduce a free-surface-tracking algorithm to analyze the filling process. There is a significant difference in heat transfer rate between the metal/mold contact point and non-contact point, and this difference in heat transfer rate affects the solidification rate of the metal. The most widely used method for free-surface tracking in mold filling is the VOF method [19]. In a two-dimensional rectangular coordinate frame, the transport equation on the VOF, F, for an incompressible fluid can be written as:

$$\frac{\partial F}{\partial t} + u\frac{\partial F}{\partial x} + v\frac{\partial F}{\partial y} = 0. \tag{5}$$

The F function governed by the above equation is unity in the fluid occupied region and zero in the empty region. For the given computational domain, the F field obtained from Eq. (5) gives the information for the free surface. The cells with F values between 0 and 1 are the free surface cells. The VOF method has been applied successfully to many engineering problems involving free surfaces including a mold filling problem. However, since the original VOF method uses an explicit differencing method in time, large computational time is required to analyze a typical filling problem due to the Courant criterion. Hence, it is more efficient to use a time-implicit VOF method to alleviate the severe time step restriction. The time-implicit VOF method [8,20] is based on the assumption that a cell being filled cannot transmit fluid to its neighboring cells until it is completely filled. Once the cell is filled, it can transmit fluid to neighboring cells. This assumption can be implemented in Eq. (5) by adopting the upwind scheme explained below.

The new modified VOF equation can be written with the conditions shown in Eq. (7) as follows [8]:

$$\frac{\partial F}{\partial t} + u\frac{\partial G}{\partial x} + v\frac{\partial G}{\partial y} = 0, \tag{6}$$

$$G = 0 \quad \text{if } F < 1, \tag{7a}$$

$$G > 0 \quad \text{if } F = 1. \tag{7b}$$

3. Numerical modeling

3.1. Filling process

The numerical method used to analyze fluid flow and thermal behavior during and after filling in the mold is described as follows. Continuity, momentum, energy and F-transport equations are discretized using the fully implicit method in time. First, the velocity and pressure fields are obtained from the momentum and continuity equations. Then the new fluid configuration is computed from Eqs. (6) and (7). The energy equation is solved for the fluid-occupied region to determine the temperature and the liquid fraction. The updated values of F are utilized to modify the velocity and pressure, and then the temperatures and liquid fractions are updated based on the modified velocity and pressure. This iteration procedure is repeated until the total fluid volume change and temperature change are small enough to satisfy the prescribed convergence criteria. If the convergence criteria are satisfied, the time is advanced. During the filling stage, the modified filling algorithm described in the previous section is used. This time-implicit VOF method is adopted to reduce the tremendous computation time that is required when the original VOF method is used. The naive VOF method uses the explicit differencing method due to its inherent characteristics and this requires very small time step sizes to satisfy the Courant criterion. The time-implicit VOF method, though it is a first-order scheme, greatly saves on computation time.

Additional details of the algorithm and the comparisons of the flow front with other numerical and experimental results can be found in the literature [8,20]. Readers interested in the numerical implementation and issues such as numerical accuracy of the method may be referred to previous articles [20]. The velocity in the solidified region is suppressed through the first term on the right-hand side of Eq. (4). The value of C in Eq. (4) is set to 1.6×10^5, and 0.001 is added to the denominator to avoid it being zero [17].

3.2. Phase change analysis

The energy equation (3), written in an enthalpy form that precludes the need to track the moving phase-change interface explicitly, can be solved efficiently if a relationship between enthalpy and temperature is given. The enthalpy–temperature relation is nonlinear for many engineering problems and may have discontinuities. This makes the numerical solution difficult and convergence poor. Great effort has been devoted to the development of an efficient solution method in the analysis of solidification problems. In this study, an implicit solution technique that uses the actual slope of the enthalpy–temperature curve is employed in accordance with the implicit filling analysis.

The enthalpy can be defined as follows

$$H = (1 - f_l)\int_{T_{ref}}^{T} c_s \, d\tau + f_l \int_{T_{ref}}^{T} c_l \, d\tau + f_l h_{sl}, \tag{8}$$

where the subscripts 's' and 'l' represent the solid and liquid phases, respectively, and h_{sl} is the latent heat. If the density and specific heat are constant at each phase and the solid phase does not move, the energy equation (3) can be written as

$$\rho c \frac{\partial T}{\partial t} + \rho c \nabla \cdot [\boldsymbol{u} T] = \nabla \cdot [k \nabla T] - \rho h_{sl} \frac{\partial f_l}{\partial t}. \tag{9}$$

The source term on the right-hand side of Eq. (9) is due to phase change. A general finite difference expression of Eq. (9) is

$$a_p T_p^{m+1} = \sum a_{nb} T_{nb}^{m+1} + d[f_l^{old} - f_l^{m+1}] + b, \tag{10}$$

where a_p, a_{nb} and d are the coefficients of the discretized equation and superscripts 'old' and $m+1$ represent the previous time level and iteration number, respectively. Here, f_l^{m+1} is expanded in a Taylor series as follows

$$f_l^{m+1} = f_l^m + \left(\frac{df_l}{dT}\right)_p \left[T_p^{m+1} - T_p^m\right]. \tag{11}$$

Introducing Eq. (11) into Eq. (10) gives

$$(a_p - S_p) T_p^{m+1} = \sum a_{nb} T_{nb}^{m+1} + S_c + b, \tag{12}$$

where

$$S_p = -d\left(\frac{df_l}{dT}\right)_p, \tag{13a}$$

$$S_c = d\left[f_l^{old} - f_l^m + \left(\frac{df_l}{dT}\right)_p T_p^m\right] \tag{13b}$$

Once the slope of the liquid fraction is given, Eq. (12) is readily solved with Eqs. (13a) and (13b); then the liquid fraction is updated according to Eq. (11). This two-step procedure is known to be more efficient [21] than the apparent heat capacity method or the fictitious heat flow method. The thermophysical properties are phase-averaged. For example, the thermal conductivity can be written as follows

$$k = (1 - f_l)k_s + f_l k_l. \tag{14}$$

4. Results and discussions

4.1. Phase change aspects

The proposed modeling technique is applied and validated through the aluminum alloy solidification problem shown in Fig. 1. Liquid aluminum is cooled from an initial temperature of 700°C through the left wall, which is maintained at 500°C. The right wall is maintained at 700°C throughout the analysis and the other walls are insulated. It is assumed that latent heat is released linear to temperature during solidification, and

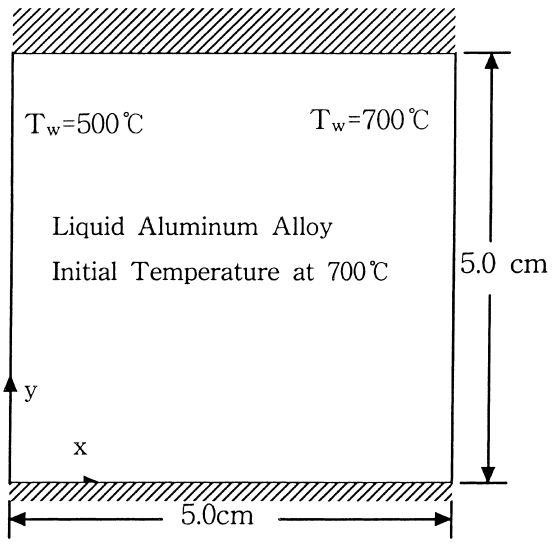

Fig. 1. Problem specification of solidification of an aluminum alloy.

hence the liquid fraction is assumed to vary linearly as follows

$$f_l = \frac{T - T_s}{T_l - T_s}, \quad T_s \leqslant T \leqslant T_l. \tag{15}$$

The thermophysical properties of aluminum used in this study are summarized in Table 1. The fluid flow result from the buoyant force and the Boussinesq approximation is introduced as shown in Eq. (4). A 30×30 uniform grid system, the same as in previous work by Swaminathan and Voller [21], is used in the computation. For this problem, the value of C is assigned to be 1.6×10^5.

Fig. 2 compares the results of this study and those of Swaminathan and Voller [21]. Fig. 2(a) is the result obtained by Swaminathan and Voller [21], and Figs. 2(b) and (c) show the present results at $t = 20$ and 30 s, respectively. The isotherms are 25°C apart, and T_s and T_l represent the solidus and liquidus lines, respectively. A direct comparison is impossible since any comment on time and the value of C could not be found in their paper; however, we have achieved a qualitative agreement with their results. The solidification of a steel ingot [22] has also been analyzed for quantitative comparison. Fig. 3 shows the temperature history of the isothermal solidification of a steel ingot. The discrepancy between the present results and those of Swaminathan and Voller [22] may stem from the artificial solidification range used in this study.

Table 1
Thermophysical properties of an aluminum alloy

Conductivity, k	100.0 W/m/°C
Specific heat, c	1000.0 J/kg/°C
Density, ρ	2500.0 kg/m^3
Liquidus temperature, T_l	650.0°C
Solidus temperature, T_s	550.0°C
Latent heat, h_{sl}	400.0 kJ/kg
Viscosity, μ	0.0025 kg/m/s
Coefficient of thermal expansion, β	4.0×10^{-5}/K

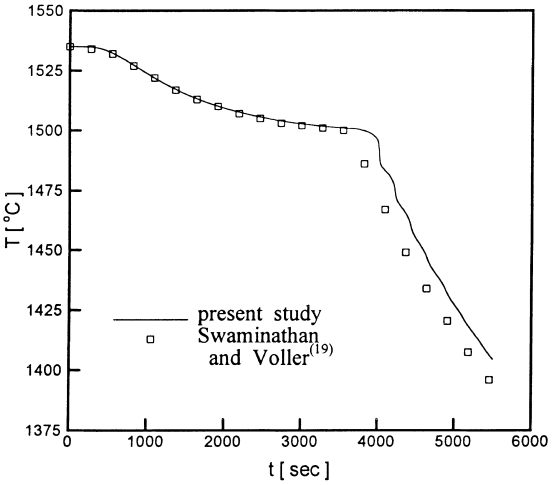

Fig. 3. Temperature history at the center of the domain of the isothermal solidification of a steel ingot.

4.2. Unified analysis of filling and solidification

The proposed unified algorithm for modeling simultaneous filling and solidification is applied to the square mold shown in Fig. 4. Liquid metal enters through the gate at the right-hand corner of the top wall, and the three walls are insulated except for the left wall. The left wall temperature is maintained at 500°C throughout the process and the gate velocity is 0.1 m/s. The Reynolds number based on the gate width is 1000. The properties of the metal are the same as in the previous problem. Fig. 5 shows the filling pattern and solidification process with time. The two isothermal lines are the solidus and liquidus lines corresponding to 550°C and 650°C, respectively. Before it hits the left mold wall (maintained at 500°C), the liquid metal does not lose its heat since there is no cooling effect. The hot metal cools as soon as it hits the left wall, which is maintained at a low temperature as shown in Fig. 5(b) ($t = 1.0$ s). At $t = 1.5$ s, it is shown that the metal is solidified from the left wall.

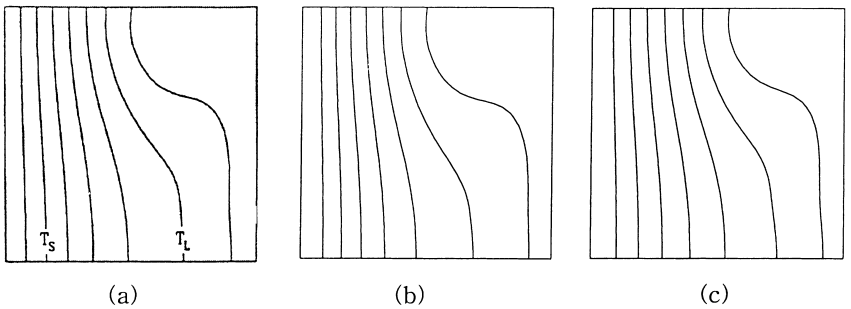

Fig. 2. Solidification of an aluminum alloy in the presence of natural convection by (a) Swaminathan and Voller [21], (b) the present study at $t = 20$ s and (c) the present study at $t = 30$ s.

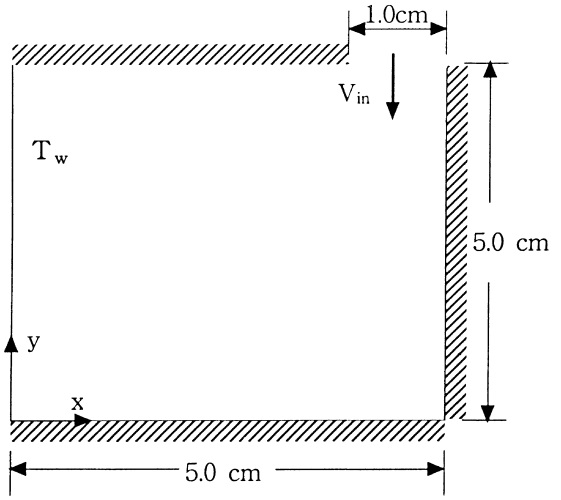

Fig. 4. Schematics of a problem for filling and solidification.

Hence, it is found that the assumption of a uniform temperature field in the mold when it is filled is not correct. Fig. 6 shows the streamlines and the progress of the solidus and liquidus lines at $t = 2.5$, 5.0 and 7.5 s, after the mold is completely filled. The liquid metal in the upper part solidifies faster than that in the lower part due to the cold upstream flow near the left mold wall. It can be seen that in the upper part of the mold, the progress of the solidus line is retarded due to the secondary flow. The secondary flow develops with the progress of solidification. Such phenomena do not occur when the filling stage is not included in the analysis. The flow field in the mushy region, though its shape and intensity may be affected by a modeling technique, has great importance since it has effects on segregation during solidification process.

Fig. 7 shows the streamlines and the progress of the solidus and liquidus lines when the temperature of the left mold wall is lowered to 400°C. The results of the filling process are not presented here because they are similar to those of the previous problem, shown in Fig. 5. The flow field shows little difference compared to that in Fig. 6, but the solidification process is much faster. When compared to Fig. 6(b), the progress of the velocity of the solidus line is faster than that of the liquidus line, and the mushy region is small since the cooling effect is dominant over the fluid flow.

The flow direction due to the filling, shown in Figs. 5–7, is opposite to that of the buoyancy driven flow. In order to analyze the fluid flow characteristics and solidification process when the inflow and the buoyancy-induced flow have the same direction, the gate position is changed to the bottom mold ($y = 0$). The x-coordinate of the gate is not changed and the temperature of the left wall is assumed to be 500°C. Shown in Fig. 8 are the flow field and two isothermal lines corresponding to the solidus and liquidus temperatures with time for this case after the mold is filled. When compared to Fig. 6, the mushy region is bulged in the lower part of the mold and the size of the secondary flow is larger. The secondary flow develops faster than in the case of the opposite flow direction because the inflow direction is the same as the buoyancy-driven-flow direction. The Grashof number is 9.8×10^6 if the left wall temperature is 400°C. The ratio of the Grashof number and the Reynolds number squared based on the mold length,or the Richardson number, is 0.4, and this implies weak natural convection effect. However, under this weak natural convection situation, the mushy region develops faster when the two flow directions are the same. Hence, the natural convection effect is not negligible. The natural convection effect due to residual flow in the mushy region is notable because the magnitude of the velocity in the mushy region is relatively small compared to that of the liquid region.

Fig. 9 shows the solidus and liquidus lines for the three different cases according to whether natural convection and filling are included or not. The mold is bottom-filled and the left mold wall temperature is assumed to be 500°C. For the pure natural convection case, the problem is solved from 2.5 s, the time when the mold is completely filled, to compare the fluid flow effects with the filling case. The liquidus line from the analysis where only natural convection is considered

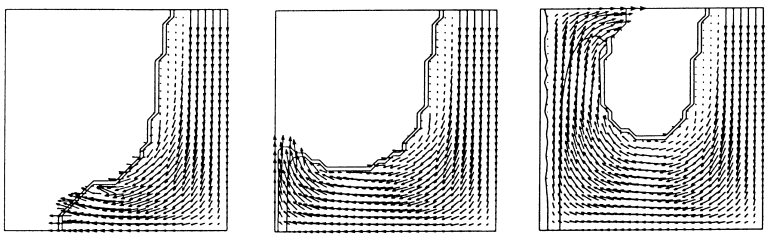

Fig. 5. Results for simultaneous filling and solidification at $T_w = 500$°C and $v_{in} = 0.1$ m/s. (a) $t = 0.75$ s, (b) $t = 1.0$ s and (c) $t = 1.5$ s.

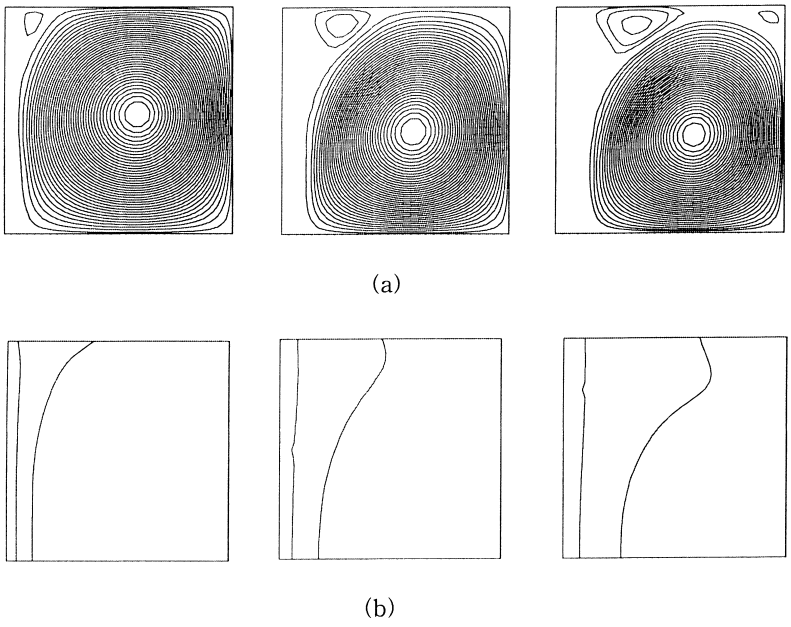

Fig. 6. Results for simultaneous filling and solidification after the mold was completely filled, in the case of a wall temperature of 500°C and an inlet velocity of 0.1 m/s. (a) Streamlines at $t = 2.5$, 5.0 and 7.5 s; (b) progress of the liquidus and solidus lines at $t = 2.5$, 5.0 and 7.5 s.

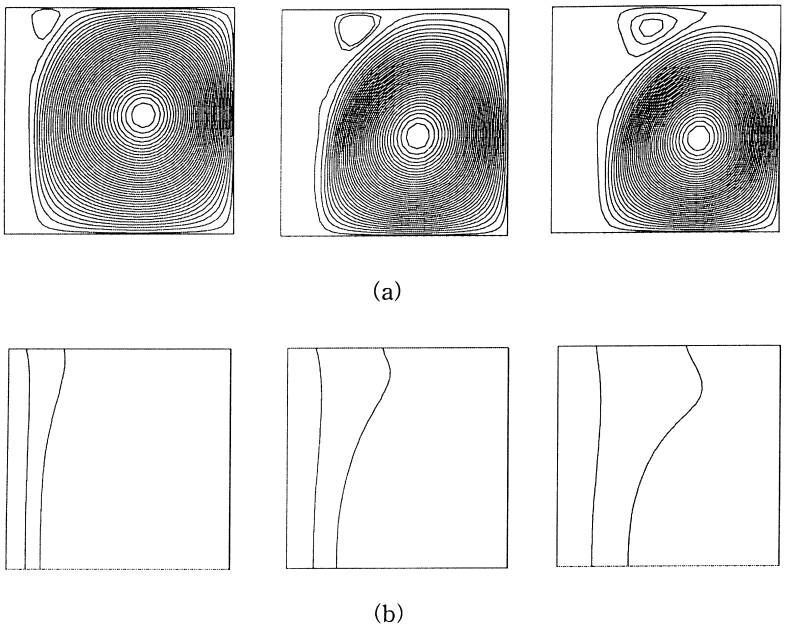

Fig. 7. Results for simultaneous filling and solidification after the mold was completely filled, in the case of a wall temperature of 400°C and an inlet velocity of 0.1 m/s. (a) Streamlines at $t = 2.5$, 5.0 and 7.5 s; (b) progress of the liquidus and solidus lines at $t = 2.5$, 5.0 and 7.5 s.

(without the filling stage) shows quite a difference when compared to the liquidus lines from the analyses where filling is considered. The liquidus line for the case with both filling and natural convection shows a stronger convection effect than in the case where filling is considered independently. From these results, it is shown

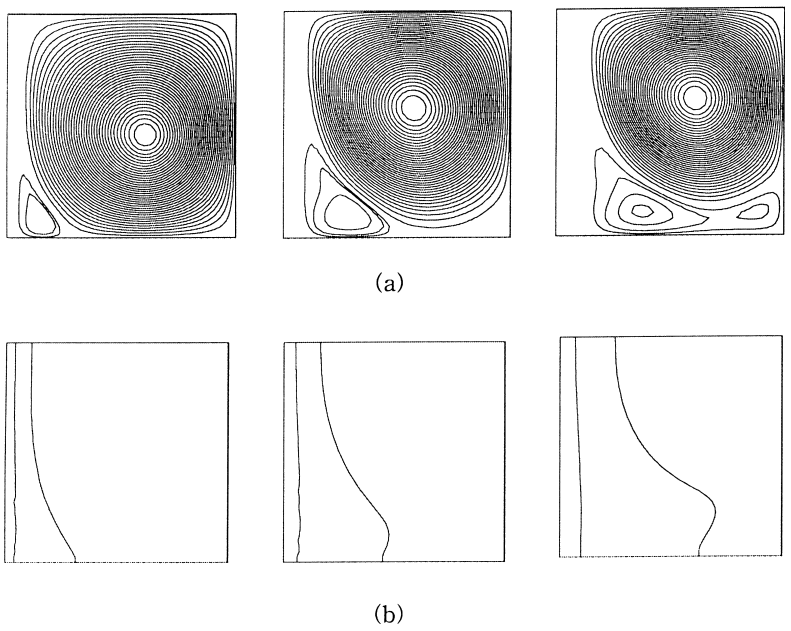

Fig. 8. Results for simultaneous filling and solidification after the mold was completely filled, in the case of bottom filling and a wall temperature of 500°C. (a) Streamlines at $t = 2.5$, 5.0 and 7.5 s; (b) progress of the liquidus and solidus lines at $t = 2.5$, 5.0 and 7.5 s.

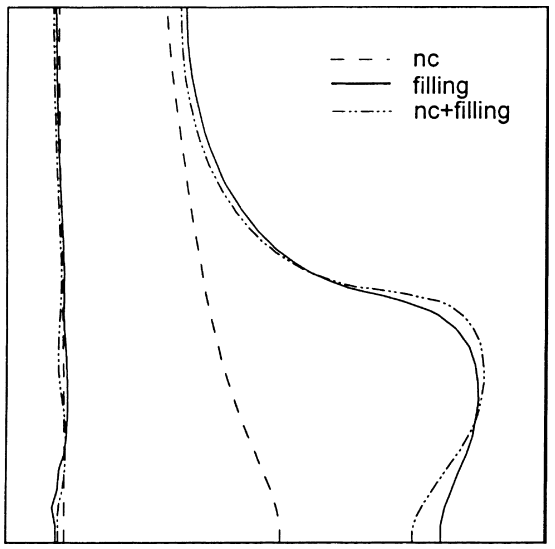

Fig. 9. Solidus and liquidus lines for three different cases with the gate located at the right corner of the bottom wall (nc: natural convection only, filling: filling only, nc + filling: both filling and natural convection).

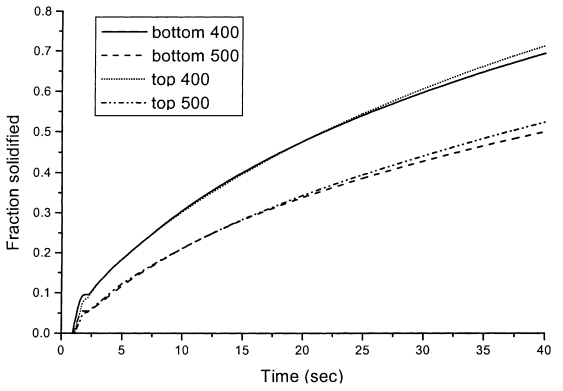

Fig. 10. Solidified volume fraction with time for the different gate positions and wall temperatures.

that the fluid flow effects due to the filling stage have to be included in the casting process analysis to predict more realistic flow patterns.

Shown in Fig. 10 is the solidified volume fraction with time for the gate position and wall temperature variation. The liquid metal is filled from the bottom or top of the mold according to the gate position. Two different mold wall temperature cases of 400°C and 500°C are considered. The bottom-filling case, denoted bottom, is the assisting flow situation where the flow directions of natural convection and residual flow from filling are the same. The top-filling case, denoted top, is the opposite flow situation where the two flow directions are reverse. It is shown that the progress of solidification is slightly faster in the case of the opposite flow situation (top-filling) than in the assisting flow situation (bottom-filling) for both cases. This is attributed to the more intense mixing in the mold for the assisting flow than for the opposing flow.

5. Conclusions

The overall process from the filling stage to solidification after filling in a model metal casting process has been numerically analyzed. The implicit filling algorithm is used and a compatible implicit method is applied to the energy equation. The solidification process including natural convection has been examined according to the variations of the gate positions and cooling conditions. The conclusions from the present study can be summarized as follows.

1. It is shown that a unified analysis of filling and solidification is needed to more accurately model the coupled effects of filling and solidification during the initial stages of casting. The residual flow due to the filling stage has an important effect on all the flow characteristics, but the natural convection effects cannot be neglected in the mushy region.
2. The results also indicate that the liquid metal solidifies faster in the case of the opposite flow situation than in that of the assisting flow direction if other conditions remain the same.
3. The development of the secondary flow is faster when the residual flow direction is the same as that of the natural convection flow.

Acknowledgements

This study was supported by the Korea Science and Engineering Foundation through Research Grant No. 981-1006-039-2.

References

[1] J. Crank, Free and Moving Boundary Problems, Oxford University Press, New York, 1988.
[2] M.N. Ozisik, Heat Conduction, Wiley, 1993.
[3] W. Shyy, M.H. Chen, Steady-state natural convection with phase-change, Int. J. Heat Mass Transfer 33 (1990) 2545–2563.
[4] M. Salcudean, Z. Abdullah, On the numerical modelling of heat transfer during solidification processes, Int. J. Numer. Methods Eng. 25 (1988) 445–473.
[5] C. Beckermann, H.P. Wang, L.A. Bertram, M.S. Sohal, S.I. Guceri, Transport Phenomena in Solidification, HTD-vol. 284, AMD-vol. 182, ASME, New York, 1994.
[6] W.S. Hwang, R.A. Stoehr, Fluid flow modeling for computer aided design of castings, J. Met. 22–29 October (1983).
[7] F. Muttin, T. Coupez, M. Bellet, J.L. Chenot, Lagrangian finite-element analysis of time-dependent viscous free-surface flow using an automatic remeshing technique: application to metal casting flow, Int. J. Numer. Methods Eng. 36 (1993) 2001–2015.
[8] C.R. Swaminathan, V.R. Voller, A time-implicit filling algorithm, Appl. Math. Modelling 18 (1994) 101–108.
[9] J.H. Jeong, D.Y. Yang, Finite element analysis of transient fluid flow with free surface with VOF (volume of fluid) method and adaptive grid, Int. J. Numer. Methods Fluids 26 (1998) 1127–1154.
[10] D. Kothe, D. Juric, K. Lam, B. Lally, Numerical recipes for mold filling simulation, Technical Report, LA-UR-98-2114, Los Alamos National Laboratory, 1998.
[11] H.P. Wang, E.M. Perry, An interactive parametric analysis tool for thin-walled investment casting, in: Modelling of Casting, Welding and Advanced Solidification Process V, TMS, 1991, pp. 595–602.
[12] J. Hu, E.R.G. Eckert, R.J. Goldstein, Numerical simulation of flows, heat transfer and solidification in pressure die casting, in: HTD-vol. 194, Modern Developments in Numerical Simulation of Flow and Heat Transfer, ASME, New York, 1992, pp. 67–74.
[13] C.R. Swaminathan, V.R. Voller, Numerical modelling of filling and solidification in metal casting processes: a unified approach, in: Proceedings, Numerical Methods in Thermal Problems, Swansea, U.K., 1993.
[14] R. van Tol, H.E.A. van den Akker, L. Katgerman, CFD study of the mould filling of a horizontal thin wall aluminum casting, in: Transport Phenomena in Solidification, HTD-vol. 284, AMD-vol. 182, ASME, New York, 1994, pp. 203–213.
[15] B. Minaie, K.A. Stelson, V.R. Voller, Analysis of flow patterns and solidification phenomena in the die casting process, J. Eng. Mater. Technol., Trans. of ASME 113 (1991) 297–302.
[16] B. Sirrell, M. Holliday, J. Campbell, Benchmark testing the flow and solidification modeling of Al castings, J. Met. 48 (3) (1996) 20–23.
[17] A.D. Brent, V.R. Voller, K.J. Reid, Enthalpy porosity technique for modelling convection–diffusion phase change: application to the melting of a pure metal, Numerical Heat Transfer B 13 (1988) 297–318.
[18] A.B. Rice, Numerical simulation of mold filling processes, Ph.D. Thesis, Purdue University, 1993.
[19] C.W. Hirt, B.D. Nichols, Volume of fluid (VOF) method for the dynamics of free boundaries, J. Comput. Phys. 39 (1981) 201–225.
[20] I.-T. Im, W.-S. Kim, Analysis of a mold filling using an implicit SOLA-VOF, Numerical Heat Transfer A 35 (1999) 331–342.
[21] C.R. Swaminathan, V.R. Voller, On the enthalpy method, Int. J. Numer. Methods Heat Fluid Flow 3 (1993) 233–244.
[22] C.R. Swaminathan, V.R. Voller, A general enthalpy method for modelling solidification processes, Metall. Trans. 23B (1992) 651–664.